AIAA JOURNAL
Vol. 41, No. 11, November 2003

Failure Prediction of Composite Lugs Under Axial Loads

Christos Kassapoglou* and William A. Townsend Jr.†
Sikorsky Aircraft, Stratford, Connecticut 06615

An approach to predict failure of composite lugs under axial loading is presented. The approach relies on superposition of the solution for an infinite plate with a pin-loaded hole and an infinite plate with an unloaded hole corrected for finite width effects based on methods presented in the literature. A relatively simple equation for the net section stress is derived. For failure prediction the maximum net section stress is equated to the first-ply failure of the laminate. The approach was used to determine analytically the optimum lug configuration. For a wide variety of layups, it was found that the optimum pin-diameter-to-lug-width ratio is approximately 0.41. A test program was executed to verify the predictions of the approach with three different lug configurations with tape, fabric, or combinations of tape and fabric materials with quasi-isotropic and orthotropic layups. The specimens were tested in tension, and in all cases the test results were within 10% of the failure predictions.

Nomenclature

$A_{11}, A_{12}, A_{22}, A_{66}$ = membrane stiffnesses of lug laminate
At = net-section area $t(w - D)$
a = lug-hole radius
D = lug-hole diameter
F^{tu} = first-ply failure of lug laminate in tension
K_T = stress concentration factor of a finite-width plate
K_T^{∞} = stress concentration factor of an infinite plate
K_{TOH}^{∞} = stress concentration factor of an infinite plate with an unloaded hole under far field tension
Kt = tension efficiency factor for a lug
P = applied load (units of force), lb
P_{fail} = far-field applied load at failure
r = radial distance from center of lug hole
t = lug thickness
w = lug width
x = radial distance from center of lug hole at $\theta = \pi/2$
θ = angular location around lug hole
ν = Poisson's ratio for an isotropic plate
σ_a, σ_A = applied far-field stress
σ_B, σ_D = stresses corresponding to superposed solutions B and D
σ_{Bcrit} = maximum stress at edge of lug hole for problem B
σ_r = radial stress at edge of lug hole
σ_θ = stress in θ direction in polar coordinates

Introduction

LUGS are very frequently used in aerospace structures to introduce or transfer loads and to connect structural members (e.g., fuselage to landing gear). They tend to be highly loaded structural details used in primary and secondary structure. As they usually are part of a single load path, they can be critical to structural integrity and performance. For this reason ways to design, accurately analyze, and predict failure of lugs are necessary. In particular, composite lugs are of primary importance because they promise weight savings. At the same time their behavior and failure modes are significantly different from metal lugs and require special analysis accounting for the material anisotropy. In what follows, composite lugs under axial loads (see Fig. 1) failing in net section under tension will be considered.

Typically, the complexity of the problem and the interaction of failure modes (net-section failure, bearing failure, shear tear-out failure) make it necessary to analyze lugs using finite elements or boundary elements. However, less time-consuming solutions, more amenable to trade studies and design optimization, are also possible. For example, a composite lug under combined loads has been examined as a special case of the bolted joint problem[1] using anisotropic elasticity and complex variables. Also, the case of an axially loaded lug has been examined as a pin-loaded hole in a plate.[2] The aim here is to develop a simple and accurate method to predict failure of axially loaded composite lugs using previous work as the starting point.

Solution and Failure Predictions

Consider the set of superposed problems shown in Fig. 2. The plates in all four cases of Fig. 2 are considered to be large so there are no finite-width effects. Problem A is the case of a self-equilibrating pin-loaded hole with total force P on each half of the hole. Problem D is the well-known problem of an unloaded hole in an infinite orthotropic plate under tension stress σ_A. Problems C and D are identical (mirror images), and they represent the lug problem at hand—the only difference being the plates in Fig. 2 are essentially infinite.

The load distribution in the hole in all problems is assumed to follow the standard cosine distribution typical of pin loads:

$$\sigma_r = (4/\pi)(P/Dt)\cos\theta \tag{1}$$

Problem A in Fig. 2 has been solved, for an isotropic plate, by Bickley,[3] and the solution is also given by Smith et al.[4] Problem D has been solved for anisotropic plates by Lekhnitskii[5] and Savin.[6]

By considering Fig. 2 and applying the principle of superposition, the stress σ_B for problem B along a line OO′ (which is the line along which net-section failure shown in Fig. 1 occurs) is given by

$$\sigma_B = \tfrac{1}{2}(\sigma_D - \sigma_A) \tag{2}$$

where the factor $\frac{1}{2}$ in front of the parenthesis accounts for the fact that problems B and C are identical. From Ref. 4 the stress σ_θ is

Received 14 February 2003; revision received 25 June 2003; accepted for publication 26 June 2003.

*Senior Structures Research Analyst, MS 352A, 6900 Main Street. Senior Member AIAA.
†Principal Structures Engineer, MS 352A, 6900 Main Street.

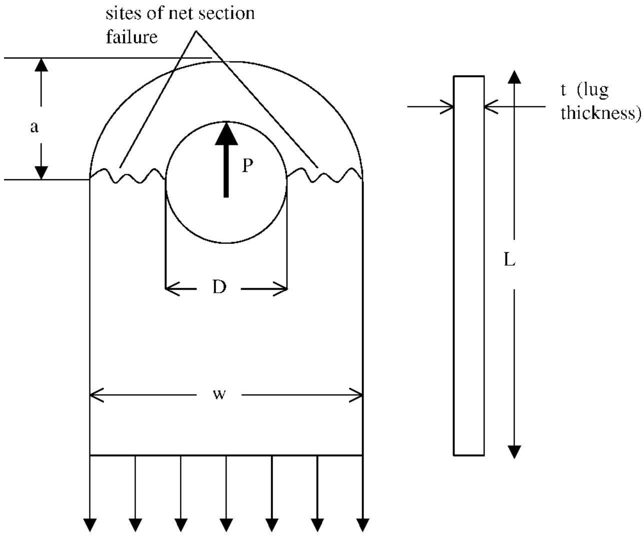

Fig. 1 Composite lug under axial load.

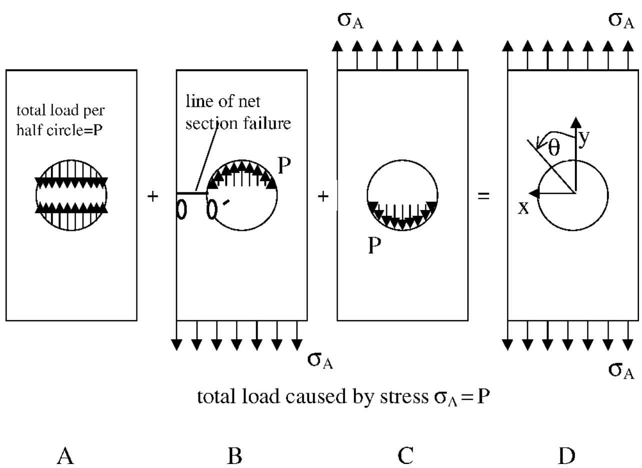

Fig. 2 Superposition of known problems to solve the problem of the pin-loaded hole.

given by

$$\sigma_\theta = \frac{2P}{\pi^2 Dt}\left(3+\frac{a^2}{r^2}\right) + \frac{(1-\nu)P}{2\pi Dt}\frac{a}{r}\cos\theta\left(1+\frac{a^2}{r^2}\right) - \frac{P}{\pi^2 Dt}\frac{r}{a}\cos\theta\left(3+\frac{a^4}{r^4}\right)\tan^{-1}\left(2\frac{a}{r}\cos\theta \Big/ 1-\frac{a^2}{r^2}\right) - \frac{P}{2\pi^2 Dt}\frac{r}{a}\sin\theta\left(3-\frac{2a^2}{r^2}-\frac{a^4}{r^4}\right) \times \ln\left(1+\frac{2a}{r}\sin\theta+\frac{a^2}{r} \Big/ 1-\frac{2a}{r}\sin\theta+\frac{a^2}{r^2}\right) \tag{3}$$

which, evaluated at $\theta = \pi/2$ (see Fig. 2), gives the stress σ_a along line OO′ for problem A. This involves a limiting procedure for the third term in Eq. (3) because the arctangent term goes to infinity and the cosθ term multiplying it goes to zero. This is accomplished with the use of L'Hospital's rule and gives

$$-\sigma_A = \frac{2P}{\pi^2 Dt}\left(3+\frac{a^2}{x^2}\right) - \frac{P}{2\pi^2 Dt}\frac{x}{a}\left(3-2\frac{a^2}{x^2}-\frac{a^4}{x^4}\right) \times \ln\left(1+2\frac{a}{x}+\frac{a^2}{x^2} \Big/ 1-2\frac{a}{x}+\frac{a^2}{x^2}\right) \tag{4}$$

where a is the radius of the hole of diameter D and t is the thickness of the plate. For future reference, it should be noted that at the hole edge ($a/x = 1$) successive application of L'Hospital's rule shows that the second term in Eq. (4) tends to zero.

For problem D the approximate, but very accurate, solution by Tan[7] is used. With some manipulation the stress σ_D along line OO′ (see Fig. 2B) is found to be

$$\sigma_D = \sigma_a\left[1+\frac{1}{2(x/a)^2}+\frac{3}{2(x/a)^3} - \frac{\left(K_{\mathrm{TOH}}^{\infty}-3\right)}{2}\left(\frac{5}{(x/a)^6}-\frac{7}{(x/a)^8}\right)\right] \tag{5}$$

where $K_{\mathrm{TOH}}^{\infty}$ is given by

$$K_{\mathrm{TOH}}^{\infty} = 1+\sqrt{\frac{2}{A_{22}}\left(\sqrt{A_{11}A_{22}}-A_{12}+\frac{A_{11}A_{22}-A_{12}^2}{2A_{66}}\right)} \tag{6}$$

where Aij are membrane stiffnesses for the laminate.

Note that with Eq. (6) material anisotropy is accounted for in this problem, unlike problem A where the solution given by Eqs. (3) and (4) is for an isotropic plate.

Combining Eqs. (4) and (5) in Eq. (2), the sought-for stress distribution along line OO′ is given by

$$\sigma_B = \frac{1}{2}\left[\begin{array}{l} \sigma_a\left\{1+\frac{1}{2(x/a)^2}+\frac{3}{2(x/a)^3} - \frac{\left(K_{\mathrm{TOH}}^{\infty}-3\right)}{2}\left[\frac{5}{(x/a)^6}-\frac{7}{(x/a)^8}\right]\right\} \\ +\frac{2P}{\pi^2 Dt}\left(3+\frac{a^2}{x^2}\right)-\frac{P}{2\pi^2 Dt}\frac{x}{a}\left(3-2\frac{a^2}{x^2} - \frac{a^4}{x^4}\right)\ln\left(1+2\frac{a}{x}+\frac{a^2}{x^2}\Big/1-2\frac{a}{x}+\frac{a^2}{x^2}\right) \end{array}\right] \tag{7}$$

It can be shown that the critical location (highest stress) is at the edge of the hole (point O′ in Fig. 2b). Evaluating Eq. (7) at that location [noting the limiting case mentioned earlier for the last term in Eq. (4)], the following expression is obtained:

$$\sigma_{\mathrm{Bcrit}} = \tfrac{1}{2}\left(K_{\mathrm{TOH}}^{\infty}\sigma_a + 8P/\pi^2 Dt\right) \tag{8}$$

which gives the highest net-section stress in a pin-loaded hole (problem B or C in Fig. 2) in a large (essentially infinite) orthotropic plate.

To obtain the sought-for solution for a lug, it is noted that a lug is basically a pin-loaded hole in a plate of finite width. So Eq. (8) is corrected for finite width using the expression by Tan[8]:

$$\frac{K_T}{K_T^{\infty}} = \frac{2+(1-D/w)^3}{3(1-D/w)} \tag{9}$$

In Ref. 8 Tan mentions that this correction factor is also valid for orthotropic plates with circular holes as suggested by Nuismer and Whitney.[9]

Therefore, by combining Eqs. (8) and (9) the critical net-section stress in an orthotropic lug can be obtained (after rearranging):

$$\sigma_{\mathrm{BcritFW}} = \frac{1}{2}\frac{2+(1-D/w)^3}{3(1-D/w)}\left(K_{\mathrm{TOH}}^{\infty}\sigma_a+\frac{8P}{\pi^2 Dt}\right) \tag{10}$$

Net-section failure of the lug is assumed to occur when the right-hand side of Eq. (8) equals the first-ply-failure F^{tu} of the laminate in tension:

$$F^{tu} = \frac{1}{2}\frac{2+(1-D/w)^3}{3(1-D/w)}\left(K_{\mathrm{TOH}}^{\infty}\sigma_a+\frac{8P}{\pi^2 Dt}\right) \tag{11}$$

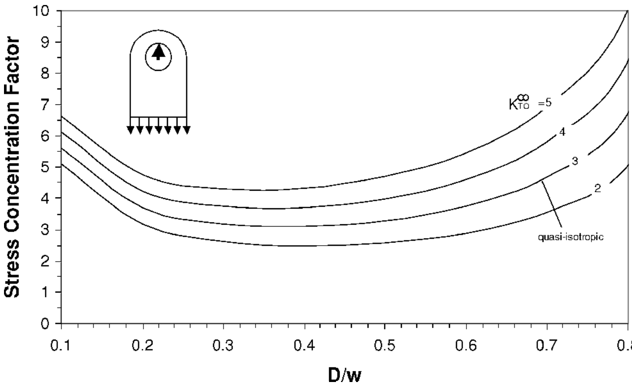

Fig. 3 Lug stress concentration factor.

Note that for a lug of finite width as in Fig. 1 P and σ_a are related through

$$\sigma_a = P/wt \tag{12}$$

so Eq. (11) can be rearranged to

$$F^{\text{tu}} = \frac{1}{2}\frac{2+(1-D/w)^3}{3(1-D/w)}\left(K^{\infty}_{\text{TOH}} + \frac{8}{\pi^2}\frac{w}{D}\right)\sigma_a \tag{13}$$

From this expression the stress concentration factor for a lug or a pin-loaded hole can be seen to equal the expression multiplying σ_a on the right-hand side. A plot of this stress concentration factor as a function of D/w for various values of the open hole stress concentration factor (infinite plate) K^{∞}_{TOH} is shown in Fig. 3.

As is seen from Fig. 3, the lug stress concentration factor decreases up to a certain value of D/w and then increases again. The presence of a minimum can be very useful in design as it gives the optimum lug configuration for a given layup (and thus value of K^{∞}_{TOH}). This behavior is caused by two opposing tendencies. At small values of D/w, the lug width is large relative to the hole diameter, and the bearing stress increases in relative magnitude and dominates the lug stress concentration factor. For large values of D/w, the bearing stress is relatively small, but the finite width effects become pronounced and dominate the behavior. Therefore, for intermediate D/w values the two effects will be less pronounced, and the stress concentration factor will go through a minimum. The exact optimum value of D/w for a given layup (K^{∞}_{TOH}) can be determined by differentiating the right-hand side of Eq. (13) with respect to D/w and setting the result equal to zero. This yields the following equation:

$$K^{\infty}_{\text{TOH}}(D/w)^5 + \left[(4/\pi^2) - 3K^{\infty}_{\text{TOH}}\right](D/w)^4 + \left[(-8/\pi^2) + 3K^{\infty}_{\text{TOH}}\right](D/w)^3 + (48/\pi^2)(D/w) - (24/\pi^2) = 0 \tag{14}$$

Solutions to Eq. (14) for various values of K^{∞}_{TOH} are given in Table 1. As is seen from Table 1 and Fig. 3, the optimum D/w value is relatively constant for a wide range of K^{∞}_{TOH} values (and therefore layups) and is very close to 0.4.

For low values of D/w ($D/w < 0.2$), the lug can fail in bearing instead of the net-section stress failure assumed here. Also, for some geometries and material properties the shear tear-out failure mode can interact with bearing failure to lead to final lug failure. Therefore, the curves in Fig. 3 and the results in Table 1 should be augmented by considering the remaining failure modes before an optimum design for a lug is generated. The geometry suggested by Table 1 would be a good start for such a design.

One additional comment on designing composite lugs under axial loads is in order. The derivation so far can be cast in a form commonly used in lug design,[10] which is based on the following equation:

$$P_{\text{fail}} = Kt\,At\,F^{\text{tu}} \tag{15}$$

Table 1 Optimum lug configuration for various K^{∞}_{TOH} values

K^{∞}_{TOH}	D/w
2	0.444
3	0.422
4	0.403
5	0.388

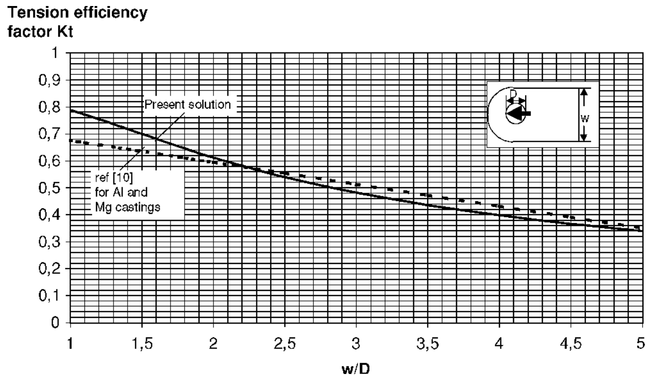

Fig. 4 Comparison of analytically obtained tension efficiency factor to the traditionally used design curve for castings.

where P_{fail} is the failure load for the lug (units of force) and F^{tu} is the failure stress of the material (or yield stress if the load at which the lug yields is required).

Equation (13) can be recast in a form analogous to that of Eq. (15). Then, the tension efficiency factor Kt is found to be

$$Kt = 6\left(\frac{w}{D}\right)^3 \Big/ \left[2\left(\frac{w}{D}\right)^3 + \left(\frac{w}{D}-1\right)^3\right]\left(K^{\infty}_{\text{TOH}} + \frac{8}{\pi^2}\frac{w}{D}\right) \tag{16}$$

Reference 10, based on the work by Cozzone et al.,[11] provides graphical representations for Kt for various metal alloys. Equation (16) was derived for a composite. However, if K^{∞}_{TOH} is set equal to 3, Eq. (16) should be close to the metal curves in Refs. 10 and 11 provided the alloys have limited yielding. Such is the case of magnesium and alloy castings. A comparison between Eq. (16) and the curve in Ref. 10 for magnesium and alloy castings is given in Fig. 4.

The two curves in Fig. 4 are in very good agreement, which provides confidence on the accuracy of the present method.

Test Results and Comparison with Theoretical Predictions

Relatively thick lug specimens were fabricated using IM7/8552 tape and fabric prepreg materials. With reference to Fig. 1, $L = 19.0$ cm (7.5 in.), $w = 5.1$ cm (2.0 in.), and $D = 2.54$ cm (1.0 in.) for all specimens. The layup and thickness are shown in Table 2. Four replicates were tested from each layup. In all specimens the pin diameter was 2.54 cm (1.0 in.). All tests were done at room temperature ambient conditions. The maximum coefficient of variation (standard deviation divided by the mean) recorded was 4.5%.

The straight end of each specimen was gripped in a materials testing system testing machine. At the other end a pin/clevis configuration was used to grip the specimen. The specimens were loaded to failure, nominally at 8.9-kN (2000-lb) intervals. Whenever there was audible damage, the test was also halted temporarily for visual inspection. At the end of each load interval, the test was stopped, and the specimen was monitored under load for any edge delaminations, brooming at the pin, or other form of visible or audible damage. Load vs stroke was recorded during each test. All of the load vs stroke plots were almost linear to failure. Near failure, the plots deviated from linearity, and audible damage was recorded. A typical load vs stroke plot for specimen F-A-1 is shown in Fig. 5.

All specimens exhibited a net-section tension failure (see Fig. 1 for location). Typical failure modes are shown in Fig. 6. Because

Table 2 Lug specimen configuration

Specimen designation	Material	Layup	t, cm (in.)
T-A	Unidirectional tape	Quasi-isotropic:	0.975 (0.384)
F-A	Fabric	Quasi-isotropic:	0.991 (0.390)
TF-A	Unidirectional tape and fabric	41/43/16: (%0/%45/%90)	0.968 (0.381)

Table 3 Composite lugs under axial loads: predictions vs test results

Layup	t, cm (in.)	$K^{\infty}_{\mathrm{TOH}}$	F^{tu}, first ply failure,[a] MPa (psi)	Test failure,[b] kN (lb)	Failure prediction, kN (lb)	% difference fm test
QI tape	0.975 (0.384)	3.00	600.1 (87,105)	97.7 (21,948)	90.9 (20,437)	−6.9
QI fabric	0.991 (0.390)	3.00	624.2 (90,590)	98.1 (22,055)	96.1 (21,587)	−2.1
41/43/16 (tape + fabric)	0.968 (0.381)	3.44	837.8 (121,601)	105 (23,686)	115 (25,869)	+9.2

[a]Using Tsai–Hill failure criterion. [b]Average of four specimens.

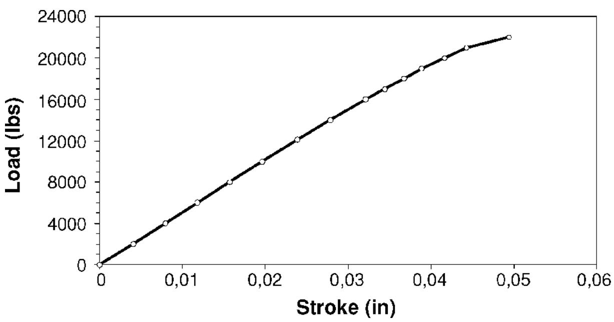

Fig. 5 Typical load vs stroke plot (fabric quasi-isotropic layup).

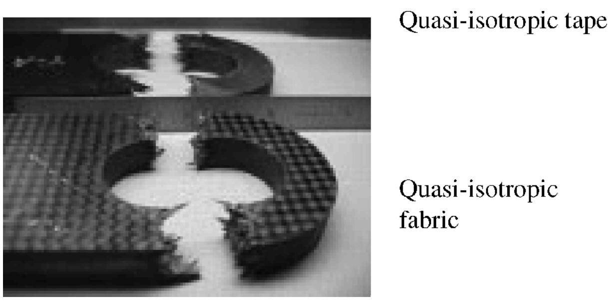

Fig. 6 Typical failure modes for composite lugs under tension.

the failure modes were tension failures at the net section, Eqs. (15) and (16) or eq. (13) can be used to predict the failure loads. The comparison of test failure loads to the predicted values is given in Table 3. Equation (16) was also used to determine $K^{\infty}_{\mathrm{TOH}}$. The value of $K^{\infty}_{\mathrm{TOH}}$ is also shown in Table 3.

The predictions are in excellent agreement (within 10%) with test results. The predictions do reproduce the fact that an all-fabric quasi-isotropic lug will be slightly stronger than an all-tape quasi-isotropic lug, even though the difference between the two is well within experimental scatter. It should be kept in mind that the predictions of the present method are based on superposition. As a result, if significant nonlinearities develop as the lug approaches failure the accuracy of the present method might degrade. Because of the layups used in all of the specimens tested here, the material nonlinearities, as would be indicated by a stress/strain plot, were quite small. The main source of nonlinearity in these layups was the elongation of the lug hole. An attempt to quantify this effect was made by measuring the stroke during the tests (Fig. 5) as given by the displacement of the lug pin, which includes the specimen extension and the hole elongation. Figure 5 suggests that the nonlinearities introduced by the hole are small, and thus the approach proposed here is valid. Still, caution should be exercised in using the present approach with any configuration that might have significant nonlinear behavior.

Conclusions

A method to predict failure of composite lugs under axial loads failing in tension in the net section was presented. Tests specimens with quasi-isotropic and orthotropic layups using a mixture of tape and fabric materials were fabricated and tested. The predictions were in excellent agreement with test results (within 10%). The analytical method was also used to optimize the lug geometry. It was found that an optimum value of the pin diameter to width ratio D/w exists for which the load-carrying ability of the lug is maximized. For typical layups the optimum value was found to be around 0.41

The solution is valid for lugs with negligible a/D or t/D effects (see Fig. 1 for definition of a, D, t). The solution was derived combining the solution for an infinite plate with a hole with the solution of an internally loaded hole. The latter was based on isotropic material, and some modification might be necessary for improved accuracy and wider applicability of the present solution. The solution is based on superposition and thus will not be valid for configurations with significant material and/or geometric nonlinearities.

In the present analysis failure is assumed to occur when the stress at the hole edge exceeds the first ply failure of the laminate. This is not the traditional approach used for unloaded holes, where the stress is evaluated at a characteristic distance away from the hole edge. Other approaches can be used where failure is defined at a characteristic distance away from the edge and different first-ply-failure criteria (Tsai–Hill was used here) are used. With judicious choice at least equally accurate if not improved predictions should be obtained.

Acknowledgments

The test program in this effort was funded by the Sikorsky Aircraft Rotary Wing Structures Technology Demonstration program partially funded by the U.S. Army (Contract DAAH10-98-2-001). The analysis work was funded by the Sikorsky Aircraft Survivable Affordable Repairable Airframe Program—Phase I, partially funded by the U.S. Army (Contract DAAH10–02-0002).

References

[1]Garbo, S. P., and Ogonowski, J. M., "Effect of Variances and Manufacturing Tolerances on the Design Strength and Life of Mechanically Fastened Composite Joints," U.S. Air Force Wright Aeronautical Lab., Methodology Development and Data Evaluation, Rept. AFWAL-TR-81-3041, Vol. 1, Sec. 3, Dayton, OH, April 1981.

[2]DeJong, T., "Stresses Around Pin-Loaded Holes in Elastically Orthotropic or Isotropic Plates," *Journal of Composite Materials*, Vol. 11, May 1977, pp. 313–331.

[3]Bickley, W. G., "The Distribution of Stress Round a Circular Hole in a Plate," *Philosophical Transactions of the Royal Society of London, Series A*, Vol. 227, 1928, pp. 383–415.

[4]Smith, P. A., Ashby, M. F., and Pascoe, K. J., "Modeling Clamp-Up Effects in Composite Bolted Joints," *Journal of Composite Materials*, Vol. 21, Oct. 1987, pp. 878–897.

[5]Lekhnitskii, S. G., *Anisotropic Plates,* translated from the 2nd Russian ed. by S. W. Tsai, Gordon and Breach, 1968, Chap. 6.

[6]Savin, G. N., *Stress Concentration Around Holes*, translated by E. Gross, Pergamon, New York, 1961, Chap. 3.

[7]Tan, S. C., "Laminated Composites Containing an Elliptical Opening, I: Approximate Stress Analyses and Fracture Models," *Journal of Composite Materials,* Vol. 21, Oct. 1987, pp. 925–948.

[8]Tan, S. C., "Laminated Composites Containing an Elliptical Opening, II—Experiment and Model Modification," *Journal of Composite Materials*, Vol. 21, Oct. 1987, pp. 949–968.

[9]Nuismer, R. J., and Whitney, J. M., "Uniaxial Failure of Composite Laminates Containing Stress Concentrations," *Fracture Mechanics of Composites*, edited by G. P. Sendeckyi, American Society for Testing and Materials, Philadelphia, 1975, pp. 117–142.

[10]Bruhn, E. F., *Analysis and Design of Flight Vehicle Structures*, Jacobs Publishing, Indianapolis, IN, 1973, Chap. D1.11.

[11]Cozzone, Melcon, and Hoblit, "Analysis of Lugs and Shear Pins Made of Aluminum and Steel Alloys," *Product Engineering*, Vol. 21, 1950.

A. Palazotto
Associate Editor